

Strut-tie approach in higher strength concrete members

Autor(en): **Ramirez, Julio A.**

Objektyp: **Article**

Zeitschrift: **IABSE reports = Rapports AIPC = IVBH Berichte**

Band (Jahr): **62 (1991)**

PDF erstellt am: **23.07.2024**

Persistenter Link: <https://doi.org/10.5169/seals-47671>

Nutzungsbedingungen

Die ETH-Bibliothek ist Anbieterin der digitalisierten Zeitschriften. Sie besitzt keine Urheberrechte an den Inhalten der Zeitschriften. Die Rechte liegen in der Regel bei den Herausgebern.

Die auf der Plattform e-periodica veröffentlichten Dokumente stehen für nicht-kommerzielle Zwecke in Lehre und Forschung sowie für die private Nutzung frei zur Verfügung. Einzelne Dateien oder Ausdrucke aus diesem Angebot können zusammen mit diesen Nutzungsbedingungen und den korrekten Herkunftsbezeichnungen weitergegeben werden.

Das Veröffentlichen von Bildern in Print- und Online-Publikationen ist nur mit vorheriger Genehmigung der Rechteinhaber erlaubt. Die systematische Speicherung von Teilen des elektronischen Angebots auf anderen Servern bedarf ebenfalls des schriftlichen Einverständnisses der Rechteinhaber.

Haftungsausschluss

Alle Angaben erfolgen ohne Gewähr für Vollständigkeit oder Richtigkeit. Es wird keine Haftung übernommen für Schäden durch die Verwendung von Informationen aus diesem Online-Angebot oder durch das Fehlen von Informationen. Dies gilt auch für Inhalte Dritter, die über dieses Angebot zugänglich sind.

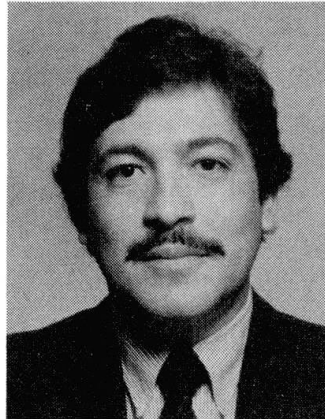
Strut-Tie Approach in Higher Strength Concrete Members

Analogie du treillis pour éléments de structures en béton
à très haute résistance

Bemessung von Bauteilen aus hochfestem Beton mit Stabwerkmodellen

Julio A. RAMIREZ

Assoc. Prof.
Purdue Univ.
West Lafayette, IN, USA



Julio A Ramirez, born 1955, received his Ph.D. in Civil Engineering from the University of Texas at Austin. Dr. Ramirez is a member of the joint ACI-ASCE Committee 445, Shear and Torsion, and the ACI Committee 408, Bond and Development of Reinforcement.

SUMMARY

The different engineering properties observed in higher-strength concretes clearly indicate the need for further basic information on the behaviour of higher-strength structural concrete. This paper makes an immediate contribution with regard to both, performance of higher-strength structural concrete and the use of strut-tie models.

RÉSUMÉ

Les différentes caractéristiques techniques que l'on observe dans les bétons à très haute résistance indiquent clairement la nécessité d'obtenir de plus amples renseignements sur le comportement de structures réalisées de la sorte. Cet article apporte donc une contribution immédiate en ce qui concerne à la fois les performances du béton à très haute résistance et l'application de modèles d'analogie du treillis.

ZUSAMMENFASSUNG

Die besonderen Materialeigenschaften von hochfesten Betonen zeigen die Notwendigkeit grundlegender Untersuchungen über das Tragverhalten von hochfestem Konstruktionsbeton. Es wird vorgeschlagen, die Methode der Stabwerkmodelle, die im Stahl- und Spannbeton eingesetzt wird, auch für die Erforschung von hochfestem Konstruktionsbeton einzusetzen.



STRUT-TIE MODEL

Strut-tie models can be formulated from experimental observations using failure crack patterns, recorded strains in the concrete and the reinforcement, together with actual specimen detailing, loading and support conditions. In design much of this information is not readily available. However, for simple everyday designs an experienced engineer is generally capable of developing strut-tie models based on common engineering sense and knowledge of the behavior of structural concrete. In the more complex design situations, this practical knowledge is often not enough to develop safe and efficient strut-tie models. In such cases, Schlaich et. al [1] suggest that the load-path method can be aided using the principal stress trajectories based on a linear elastic analysis of the structure. The principal compressive stress trajectories can be used to select the orientation of the strut members of the model. The strut-tie model can then be completed by placing the tie members so as to furnish a stable load-carrying structure.

The strut-tie approach for higher-strength concrete members is illustrated with the analysis of a pretensioned beam, specimen I-4A. This specimen was tested to failure using a point load system [2]. The detailing of the specimen is shown in Figure 1, and the material properties are given in Table 1. The strut-tie model for specimen Type I-4A shown in Figure 2(a), is developed first by placing the strut members in the direction of the principal compressive stress trajectories. Next, the vertical ties of the model are placed at the stirrup locations and the horizontal tie is located at the centroid of the strand pattern. In deep beams the usual assumption of linear distribution of strains over the depth of the section is not adequate. The capacity of this type of member in either flexure or shear depends heavily on the detailing of loading and support. This component of the load carrying mechanism, in the form of an inclined strut going from the support to the point load, is clearly shown in the failure crack pattern in Fig. 1.

The development of a strut-tie model is an iterative process because the widths of the struts and the size of the nodes depend on the forces in the struts and ties. A computer program has been developed at Purdue University to help carry out this process [3]. Initially, the truss model is laid out using the centerline dimensions of the strut and tie members. The effects of the prestressing are represented by the equivalent horizontal loads of 310.3^k (1380.2 kN) and 74.6^k (331.8 kN) shown in Figure 2(a). For the failure load analysis the maximum load of 323^k (1436.7 kN) is applied to the strut-tie model and a preliminary analysis is conducted to determine the internal forces in the individual members of the model. Next, the strut members are dimensioned using allowable compressive stresses checking that the resultant dimensions are compatible with the actual geometric constraints of the specimen. The resultant strut-tie model with finite dimensions for the strut members and nodal zones (Fig. 2b) is then analyzed for the applied load and the external forces representing the effects of prestressing. The equivalent prestressing load applied to the tension chord of the strut-tie model is updated by adding to it the force in the tie member next to the support resulting from a first analysis of the model with finite width for the initial prestress force and ultimate load. Finally, the forces in the horizontal tie member obtained from the analysis of the strut-tie model with finite width members for the applied maximum load and updated equivalent prestressing load must be added to the additional tension force calculated from the initial prestressing in order to obtain the actual tension force in the strands at ultimate load. The resultant analysis forces in the vertical ties of the model can be used directly to calculate the required tension force in the transverse reinforcement (stirrups). Next, the principal stresses in the critical nodal zones are determined using the stresses and the geometry of the individual members framing the nodes. This procedure is illustrated in the following section with the test results of specimen I-4A.

EXPERIMENTAL EVALUATION

In the determination of the strut widths of the model for beam I-4A, the compressive stress levels used were $0.9f_c$ for the diagonals going from the point load to the support, $0.3f_c$ for all other strut members, and $0.5f_c$ for the upper compression members. The selection of the stress levels is an iterative process where the measured forces in the strands at the locations shown in Figure 1 were used to refine the estimates. The geometry of the strut-tie model based on the stress levels mentioned above resulted in the calculated forces shown in Table 2. The calculated strand forces were determined using the procedure outlined in the previous section. As can be seen from Table 2, a tension force of 36 kips must be properly anchored at the support. In specimen I-4A a 2 ft. (609.6 mm) overhang on the N-side and more than 2 ft on the S-side was provided to ensure proper anchorage. At failure, no slippage of the strands was observed. The calculated forces at failure in the vertical tension ties of the strut-tie model indicated yielding of this reinforcement. This was confirmed by the strain measurements in the instrumented stirrups. First diagonal cracking in specimen I-4A occurred at a load of 236^k (1049.7 kN) yielding of the stirrup reinforcement was observed immediately after first cracking; however, no stirrup fracture was noted at failure. Failure in specimen I-4A occurred due to crushing of the concrete under the point load followed by crushing of the web section on S-side as shown by the failure crack pattern in Fig. 1. The size of the critical nodal zone under the point load is controlled by the dimensions of the struts framing into it as well as the dimensions of the bearing plate and the width of the specimen. Once the geometry was determined, a finite element analysis was carried out to determine the principal stresses. After an element grid has been laid out in the nodal zone, the axial forces in the individual struts and applied load are discretized into their components parallel and normal to the boundaries of the nodal zone and applied as concentrated loads at the nodes of the elements bordering each strut and the loading plate. Figure 3 shows the chosen finite element grid and applied boundary forces for the portion of the nodal zone where failure was observed. The results of the analysis indicated a state of biaxial compression for most of the nodal zone and a maximum principal compressive stress of 9.76 ksi (67.3 MPa) at element 90, matching the region where failure occurred.

CONCLUSIONS

The use of increased concrete strengths would produce stronger nodal zones and strut members. If the strut-tie mechanism is properly developed this would result in improved ultimate capacity. Hence, adequate detailing of the member is further emphasized with the use of higher-strength concretes. In deep beams the ultimate capacity in either flexure or shear depends heavily on the strength of the main diagonal strut and the proper detailing of loading and support regions. The loading plate determines one of the dimensions of the nodal zone under the point load and at the support, thus affecting the state of stress at the node. Proper anchorage at the support region of the longitudinal tension reinforcement is also critical for the development of the strut-tie mechanism. Although not so critical for deep beams, in more slender members with low amounts of shear reinforcement the use of higher-strength concrete could jeopardize the formation of an adequate strut-tie mechanism upon first diagonal tension cracking. Because of the increased shear force to be transferred at the onset of first diagonal tension cracking and the possible reduction of aggregate interlock contribution the higher shear force to be transferred upon diagonal cracking could cause the first mobilized stirrups to yield and rupture.



REFERENCES

1. Schlaich, J., Schafer, I., and Jennewein, M., "Towards a Consistent Design of Structural Concrete," *Journal of the Prestressed Concrete Institute*, Vol. 32, No. 3, May-June 1987, pp. 74-150.
2. Kaufman, M.K., and Ramirez, J.A., "Re-evaluation of the Ultimate Shear Behavior of High-Strength Concrete Prestressed I-Beams," *ACI Structural Journal*, V. 85, No. 3, May-June 1988, pp. 295-303.
3. Alshegeir, A., and Ramirez, J.A., "Analysis of Disturbed Regions with STRUT-TIE Models," Structural Engineering Research Report No. CE-STR-90-1, Purdue University, West Lafayette, IN, January 1990, 85 pp.

Table 1 - Type I-4A Information

TYPE I - 4A

Geometry:		Concrete:		
			Transfer	Test
Beam Length (ft)	17	f'_c (psi)	5840	8810
Test Span (ft)	10	E_c (ksi)	5620	5930
Shear Span, a (ft)	5	f_r (psi)	920	-
	$\frac{a}{d_p}$ 2.35			
Prestressing Strand:		Mild Reinforcement:		
	Top	Bottom	#5 Bar	#4 Bar
Grade	270	270	Grade 60	40
A_{ps} (in ²)	0.1633	0.1633	A'_s, A_v (in ²)	0.31 0.19
d_p, d_p (in)	2.00	26.00	d', r_{fy} (in, psi)	2.00 165
E_{ps} (ksi)	27920	27920	E_s (ksi)	29020 29500
f_{pu} (ksi)	282.0	282.0	f_y (ksi)	64 52
f_{si} (ksi)	207.6	193.3		
f_{se} (ksi)	199.9	187.8		
P_{e1}, P_{e2} (kips)	65.3	245.4		

SI Equivalents

1 in	= 25.4 mm
1 in ²	= 645.2 mm ²
1 lb	= 4.448N
1 psi	= 0.006895 MPa

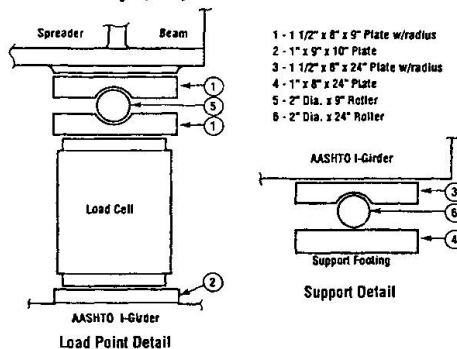


Table 2. Measured and Predicted Strand Forces (kips) for P = 323 kips

Gage #	14	13	12	11	10
Measured	36	39.03	41.75	42.48	36.7
Predicted	35.37	38.16	40.72	41.32	36.91

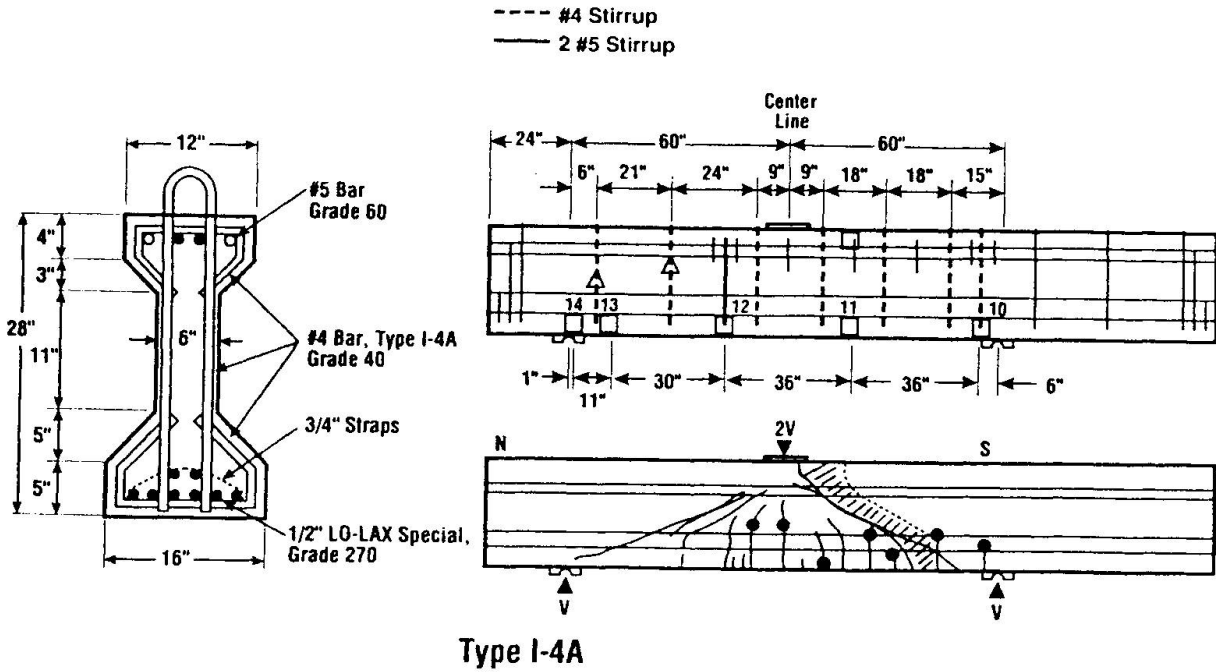


Fig. 1. Detailing and Failure Crack Pattern of I-4A.

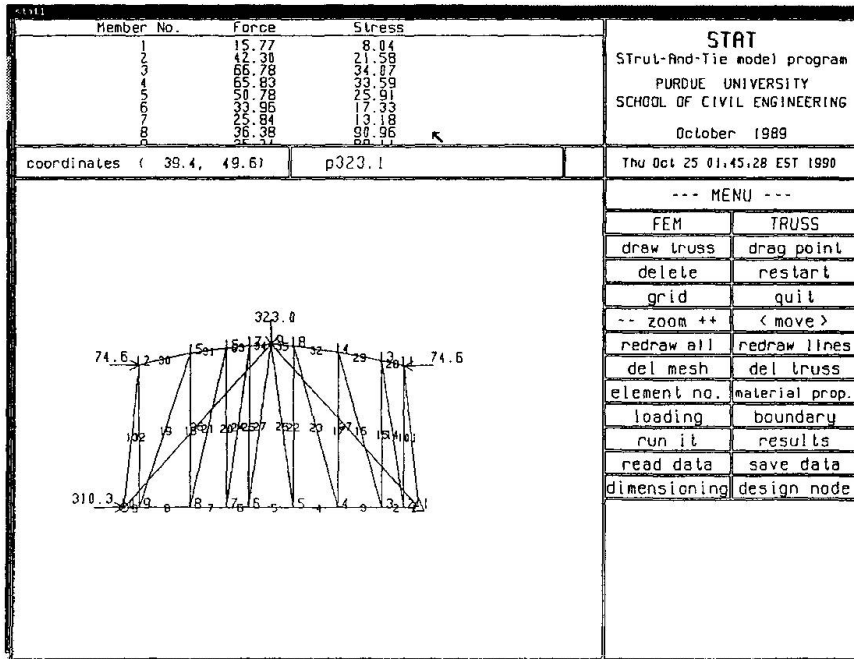


Fig. 2(a). Centerline Dimension Strut-Tie Model

